# Full-pupil versus divided-pupil confocal line-scanners for reflectance imaging of human skin *in vivo*

Dan Gareau, Sanjeewa Abeytunge, Milind Rajadhyaksha
Memorial Sloan Kettering Cancer Center, New York, NY

Contact: Dan Gareau, dan@dangareau.net

## ABSTRACT

A full-pupil confocal line-scanning microscope is under development for imaging human skin *in vivo* in reflectance. The new design potentially offers an alternative to current point- and line-scanners that may simplify the optics, electronics and mechanics, and lead to simpler and smaller confocal microscopes. With a combination of a cylindrical lens and an objective lens, the line-scanner creates a focused line of laser light in the object plane within tissue. An oscillating galvanometric mirror scans the focused line transverse to its axis. The backscattered light from the tissue is de-scanned and focused onto a linear CMOS detector array. Preliminary measurements of the axial line-spread function, with a 30x, 0.9-NA water immersion objective lens and illumination wavelength of 633 nm, determined the optical sectioning to be 10 μm. The new design is simple, requiring only eight optical components. However, the disadvantage is non-confocality in one dimension that results in 20% weaker sectioning than with a point-scanner, and reduced contrast in scattering tissue. The images of standard reflective targets such as a mirror and grating as well as dermis-like scattering target such as paper offer a preliminary glimpse into the performance of the line-scanner. A similar alternative design is the divided-pupil (theta) line-scanner, which provides 50% weaker sectioning than with a point scanner, but better contrast and less speckle due to the theta configuration. Such line scanners may prove useful for routine imaging of humans in clinical settings.

## INTRODUCTION

Instruments developed for point scanning confocal microscopy that noninvasively image skin and other tissues typically contain complex expensive optical, electrical and mechanical components. Confocal line scanning eliminates the need for two separate optomechanical scanning mirrors and promises simpler, less expensive reflectance confocal microscopy. In the two experimental apparatuses reported on here, a single galvanometric mirror scanned a focused line within the sample to create the field of view. The de-scanned conjugate of this line illuminated either a linear photodiode array detector (Perkin-Elmer, Canada, RL1024) or a slit, which acted as the confocal aperture.

The two line scanning designs are both simpler and less costly than the point scanning alternative. Their performance is under evaluation to determine whether they are competitive with the point scanning system for imaging human skin. The first design, a divided-pupil line scanning system[3], illuminates one half of the objective lens and collects from the other half. Although the divided pupil design looses optical sectioning due to its limited use of only half the numerical aperture of the objective lens, it regains performance with a superior ability to filter out multiply scattered light. The second design, a full-pupil line-scan system both illuminates and collects with the entire pupil of the objective lens. This design is attractive because it is even simpler than the divided pupil but coaxial illumination and detection leads to greater acceptance of multiply scattered light, which adversely affect performance in thick samples such as skiin.
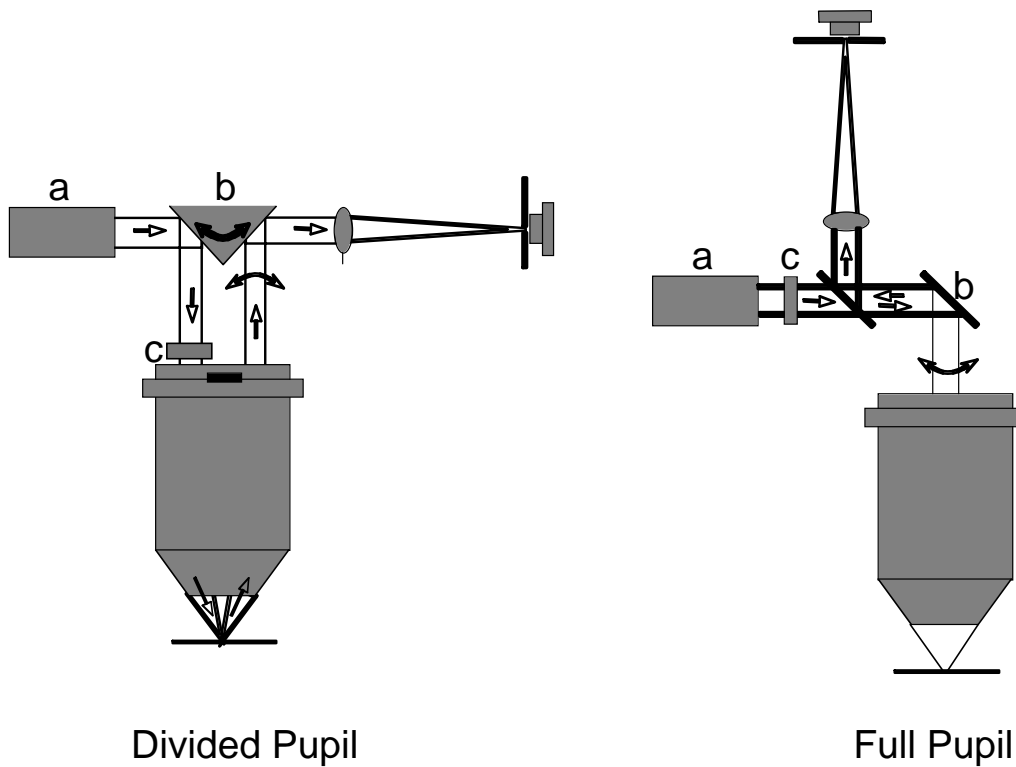
Figure 1 Comparison of divided pupil and full pupil line-scan designs. a: laser b: scanning mirror galvanometer c: cylindrical lens.

Figure 1 compares the designs of the two types of line-scanners. In the divided pupil, the cylindrical lens (c) converts the collimated laser beam into a scanned line, which is scanned through one half of the objective lens pupil. In the full-pupil design, the focal plane of the cylindrical lens is placed at the shoulder plane of the objective lens. This configuration allows for the beam to be collimated in the direction perpendicular to the focused line within the sample.

Primary evaluation of performance was made on the axial line-spread function. A mechanical translation stage (Nanomotion II, Melles Griot, 11NCS101) stepped a mirror through the focal plane while reflected light was measured through the slit aperture. It was observed that the line-spread function of the full pupil design was much poorer than that of the divided pupil so the device was critically examined.

**THEORY**

The beam splitter used in the experimental setup for the full pupil line scanner (element between c and b in the full pupil diagram in figure 1) was a 1-inch cube beam splitter. Optical sectioning was poor under this configuration so the design was critically examined. The conclusion was that the most likely weak link was the beam splitter. It was hypothesized that aberrations caused by beam splitter were corrupting the focused line within the sample. The effect of a window in the path of a focusing beam was simulated using Snell's law in Matlab for a deeper understanding of its role in determining the system's performance . The simulation included independent input variables:

1) Refractive index of the window ($n_2$) as well as the surrounding medium ($n_1$)
2) Window thickness (D) and position
3) Number of rays to launch

The two primary dependent output variables produced were the focal shift (S) and longitudinal aberration (LA), shown in figure 1b. The simulation used Snell's law at the boundary of refractive index mismatch. The simulation was independently verified by the theory laid out by Smith[1] and Wan *et al.* [2] The length of focal extension into the sample (S) is expected[1] to be:

$$S = D(1 - n_1/n_2) \tag{1}$$

Figure 2a shows the focal position (dashed line) of the converging rays (solid lines) before the optical window was inserted. Without the window in the optical path, the rays converged perfectly in the focal plane of the lens as prescribed in the simulation. With the window inserted, the refracted rays (solid lines) came to a focus at a greater distance (again, dashed lines) from the lens.

When the beams were set on initial trajectories such that they would converge at the focal length perfectly in an obstacle-free environment and the glass window was inserted, they did not converge perfectly, rather to different points along the z-axis spanning a total distance given by the longitudinal aberration. The longitudinal aberration expected[2] is given by:

$$LA = D\left( \sqrt{\frac{n_1^2 - NA^2}{n_2^2 - NA^2}} - \frac{n_1}{n_2} \right) \tag{2}$$

The results in figure 1 were produced using a lens of focal length 100 mm and height 10 mm, an optical window of D = 25.4 mm thickness, and 10 rays. The focal shift was S = 8.690 mm and the longitudinal aberration was LA = 12 μm.
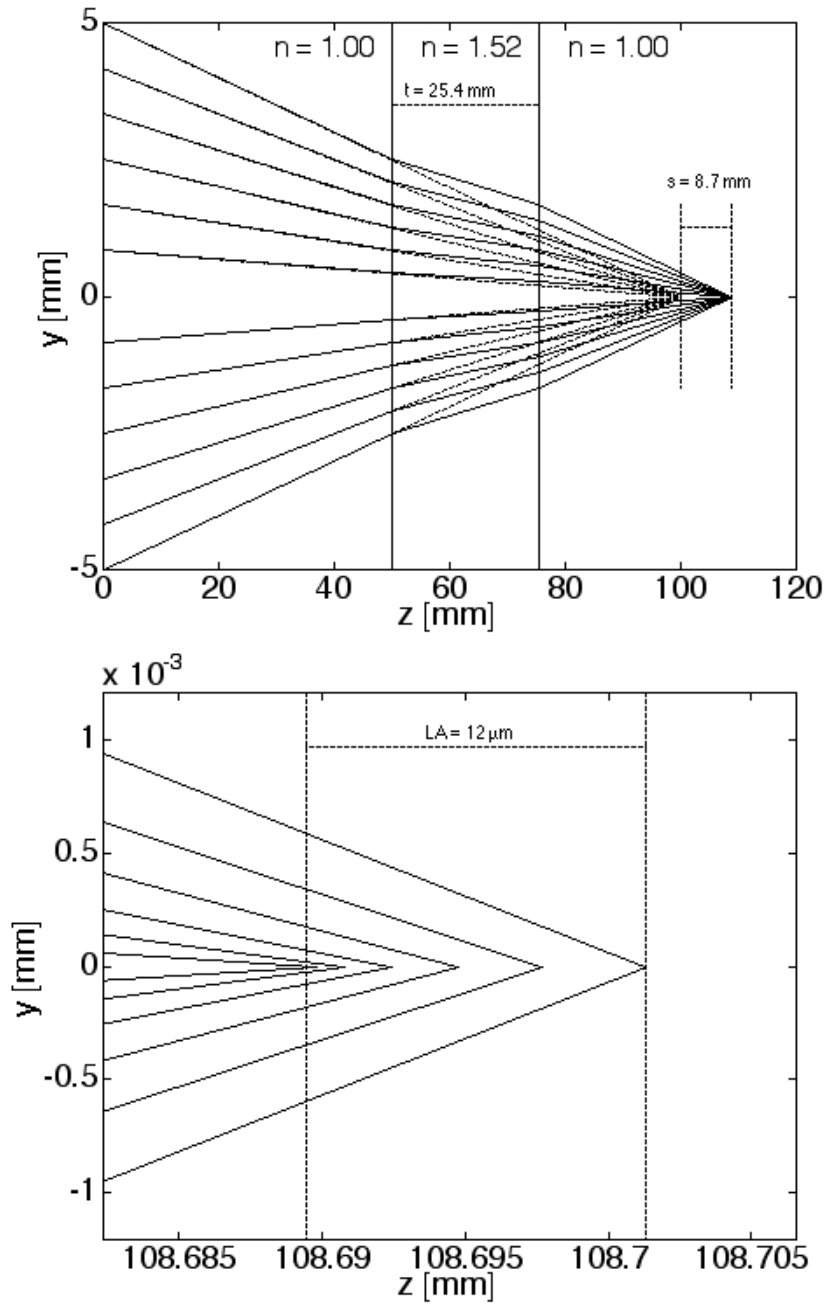
Figure 2 The ray-tracing simulation output. The top figure shows the focal shift (S) due to insertion of an optical window of thickness D. The lower figure shows a close up of the extended focal spot with window inserted.

The longitudinal aberration is expected to degrade images because it is larger than the axial optical resolution element, which is given by:

$$\Delta z = 1.4\lambda/NA^2 \tag{3}$$

Calculated for $\lambda = 633$ nm light with an objective lens numerical aperture (NA) of 0.90, the axial resolution element is $\Delta z = 1.1$ µm, about ten times smaller than LA. To directly compare the LA and $\Delta z$, one would

compute the Fourier Transform of the wave-front in the pupil plane to yield the light distribution in the object plane. This step was not completed but will be included in future work.

The glass cube beam-slpitter in the configuration was replaced with a nitrocellulose (n = 1.51) pellicle beam splitter of 2 μm thickness at 45 degrees for diminishing the LA. The ray-trace model using Snells law shows the aberrations at the focus:
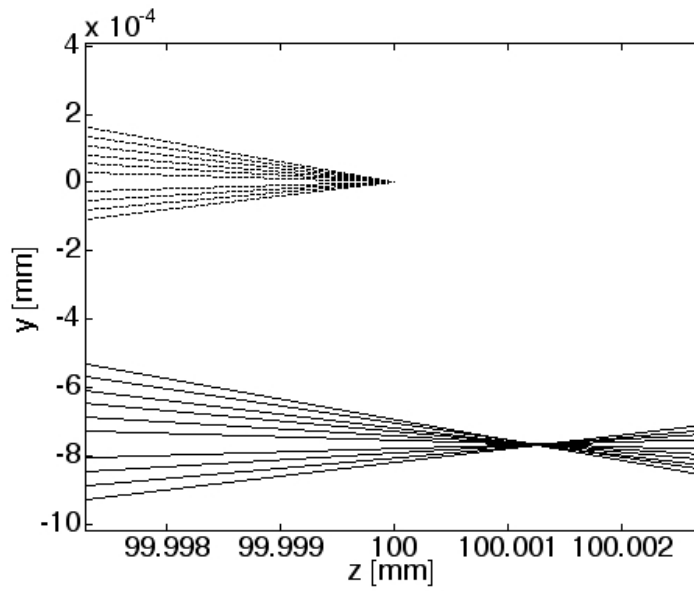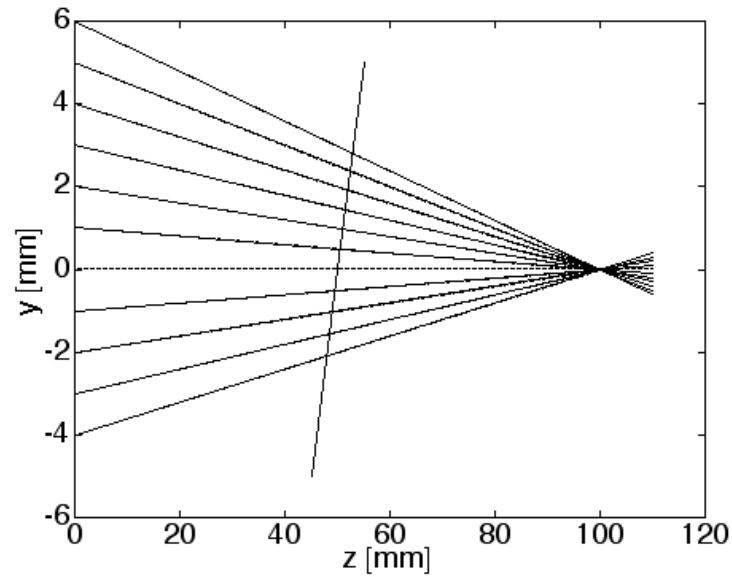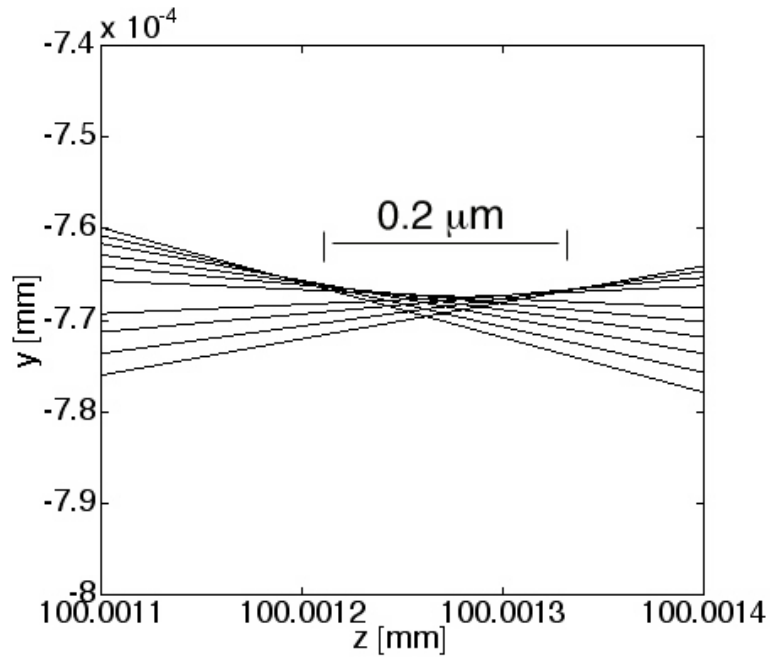
Figure 3  Ray-trace for the 45-degree pellicle membrane beam splitter placed in the path of focused light.  The middle figure is a close-up view of the focal region.  The resulting focus shifts forward and downward.  The lower figure is an extreme close up of the resulting focus.

## RESULTS

Line spread function measurements showed better performance for the divided pupil line-scanner than for the full pupil design.  The full width at half maximum for the LSF with the divided pupil was 1.7 μm while the full pupil yielded a LSF with a full width at half maximum of 10 μm.
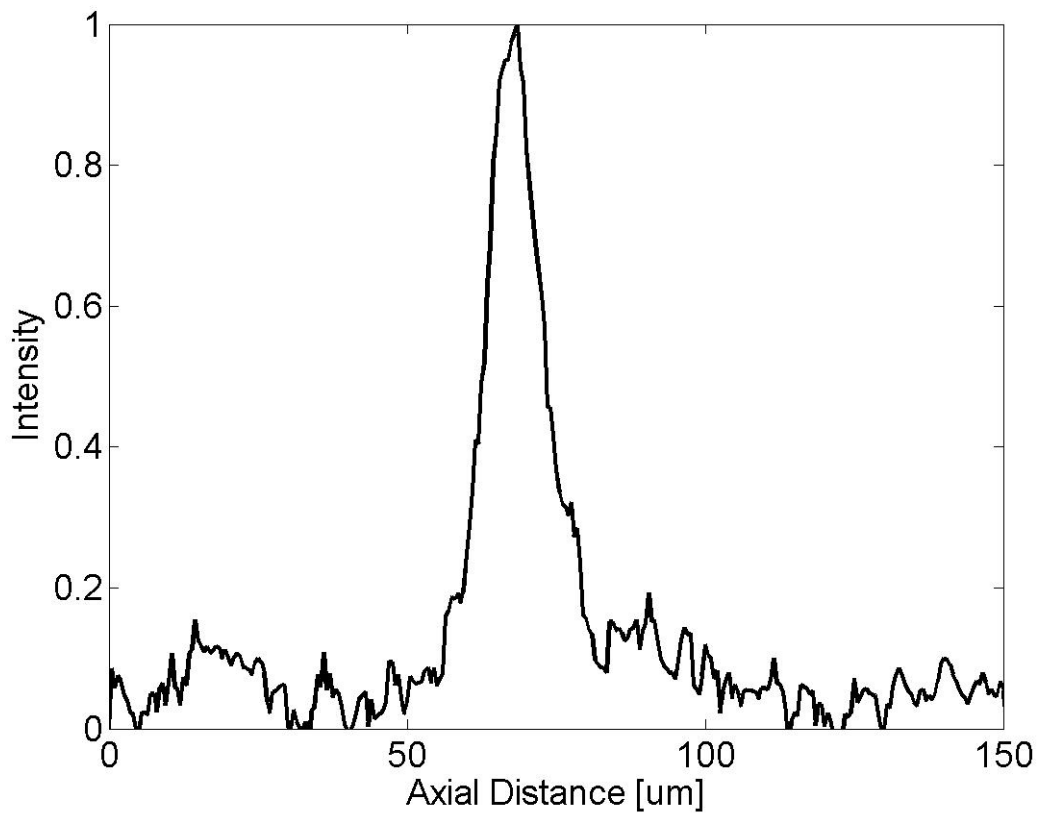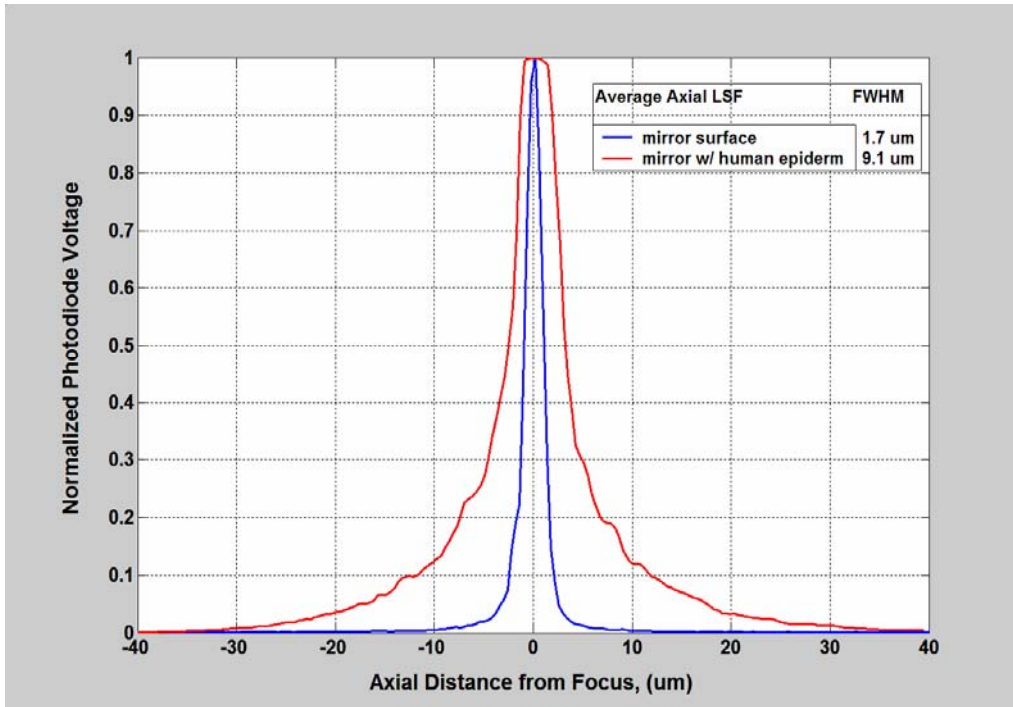
Figure 4  The axial line-spread functions for (a) the divided pupil design and (b) the full-pupil design.

Figure 4 shows the line spread functions for the two line scanning designs.  For the divided pupil, the FWHM is 1.7 μm compared to a predicted value of 1.3 μm.  For the full pupil design, the FWHM is 9.6 μm.
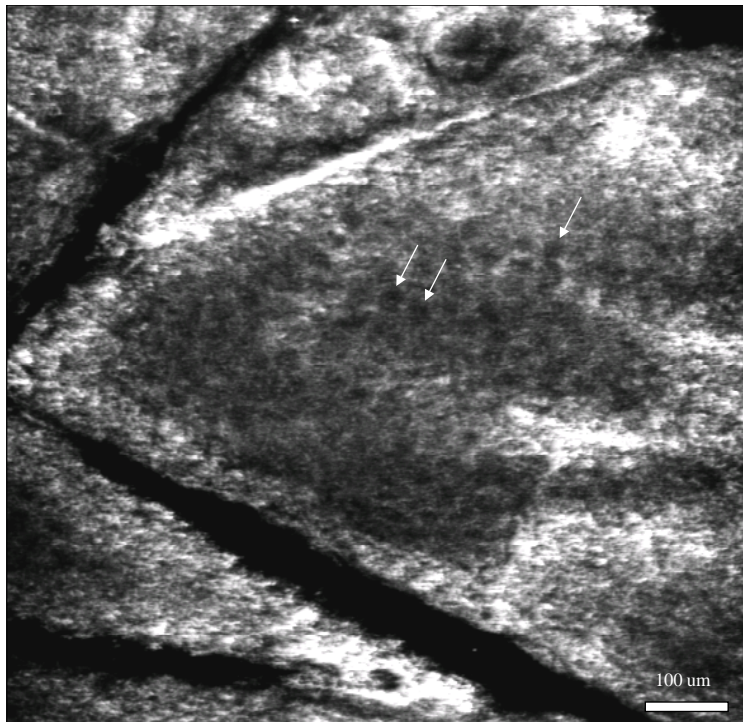


Figure 5   Skin imaged in vivo with the divided pupil line scanner.  Granular cells present with dark nuclei noted with arrows.

Figure 5 shows imaging of keratinocytes in the epidermis through the stratum corneum.  Dark nuclei appear in a honeycomb pattern.  The divided pupil was successful in imaging detail in skin while the full pupil line scanner was only successful in imaging the fibers of a paper business card.
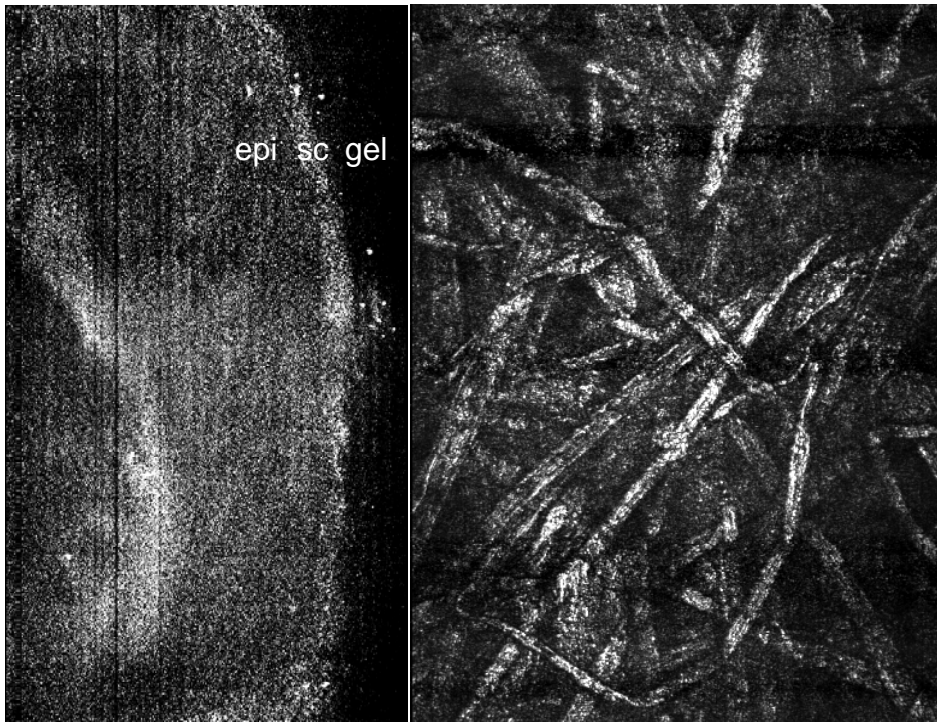
Figure 6  Full pupil line scan images of skin (left) and paper fibers (right).

## DISCUSSION AND FUTURE WORK

The performance of line scanning thus far is limited to imaging skin with the divided pupil.  Although surface images of stratum corneum and preliminary images of granular cells are encouraging, better designs must be reached before the full pupil becomes competitive with the current point scanning devices.  The divided pupil design has proven competitive[4].

Future work includes adapting the ray-trace to account for asymmetric aberrations such as astigmatism and coma.  Also, Fourier analysis will be applied to determine the light distribution in the object plane given the output of the simulations above in the pupil plane of the objective lens.

References
[1]        W. J. Smith, Modern Optical Engineering.  SPIE Press and McGraw Hill, Copyright 2000.
[2]        Wan D.-S., Rajadhyaksha M., Webb R.H., Analysis of spherical aberration of a water immersion objective: application to specimines with refractive indices 1.33-1.40, Journal of Microscopy **197:**274-284, 2000.

[3]  Dwyer P.J., DiMarzio C.A., Fox W.J., Zavislan J.M., Rajadhyaksha M., Confocal reflectance theta line-scanner for imaging tissues in vivo, Proceedings of SPIE, **5701:**116-121, 2005.
[4] Dwyer P.J., DiMarzio C.A., Zavislan J.M., Fox W.J., Rajadhyaksha M., Confocal reflectance theta line scanning microscope for imaging human skin in vivo, Optics Letters, **31:**942-944, 2006.